Annales Geophysicae (2005) 23: 75–85
SRef-ID: 1432-0576/ag/2005-23-75

Annales Geophysicae

Observations of time dependence and aspect sensitivity of regions of enhanced UHF backscatter associated with RF heating

R. S. Dhillon and T. R. Robinson

Department of Physics and Astronomy, University or Leicester, University Road Leicester, LE1 7RH, UK

Received: 20 February 2004 – Revised: 30 April 2004 – Accepted: 18 May 2004 – Published: 31 January 2005

Part of Special Issue "Eleventh International EISCAT Workshop"

Abstract. The EISCAT incoherent radar system, which is collocated with the EISCAT heating facility, is used to diagnose the ionosphere while heating experiments are conducted. In late September 2002, an experiment was performed in which the heater transmitted a 2-min-on/2-min-off cycle while its pointing direction was kept fixed and the UHF beam was cycled through five pointing directions. This UHF cycle was used for three heater beam-pointing directions. For field-aligned heater beam and UHF pointing, UHF data indicated a gradual decrease, with time, in the altitude at which enhanced ion-line scatter occurred. This was accompanied by a reduction in the intensity of the scatter. For field-aligned heater pointing and the UHF elevation angle of 6° in the field-aligned direction, a persistent high-amplitude signature was observed, which remained at a fairly constant altitude throughout the period that the heater remained switched on. Different time histories of the backscatter amplitude were observed in other UHF pointing directions, including the "ion-line overshoot", which is characterized by an increase and subsequent decrease in the heater-enhanced backscatter just after heater switch-on. It is suggested that these signatures may be caused by the presence or absence of field-aligned irregularities and reduced recombination caused by heating. The CUTLASS coherent radar system, which operated simultaneously with the UHF radar and the heater, observed backscatter from field-aligned irregularities created by the heater. The intensity of this backscatter was highest from the regions of the ionosphere that were excited by the central part of the heater beam.

Key words. Ionosphere (Active experiments; auroral ionosphere, wave propagation)

1 Introduction

Among the most important features of experiments in which ordinary-mode (O-mode) high power radio (heater) waves are transmitted into the ionosphere and interact with the ionospheric plasma are the stimulation of small-scale electrostatic waves and non-propagating plasma density irregularities (e.g. Robinson, 1989; Rietveld et al., 1993; Kohl et al., 1993; Mishin et al., 2004). The density irregularities tend to be field-aligned in the ionosphere, because of anisotropic electron transport effects. Thus, these irregularities commonly produce strong backscatter in radars with beams directed perpendicular to the geomagnetic field, towards the interaction region (e.g. Hedberg et al., 1983; Coster et al., 1985; Bond et al., 1997; Dhillon et al., 2002; Kolesnikova et al., 2002).

Heater-excited plasma instabilities lead to coupling between the electromagnetic pump wave and (a) electron-acoustic and ion-acoustic waves at the reflection height and (b) upper-hybrid/electron-Bernstein and lower-hybrid waves at the upper-hybrid height (e.g. Istomin and Leyser, 1995). Within certain limitations, the ion-acoustic or electron-acoustic waves are fairly isotropic and can be detected in the interaction region by radars pointing in all directions, including those close to the geomagnetic field direction (e.g. Stubbe et al., 1992; Kohl et al., 1993; Djuth et al., 1994; Isham et al., 1999; Honary et al., 1999; Rietveld et al., 2000). These quasi-isotropic wave types give rise to enhancements in the characteristic ion-line and plasma-line incoherent scatter spectra, respectively. Although the two types of scatter (field-perpendicular and quasi-isotropic) described above occur simultaneously after a heater wave is turned on, the two types of radar observation have largely been made independently. However, in the experiments described below, which were conducted with the EISCAT heater at Tromsø, Norway, the CUTLASS (Co-operative UK Twin Located Auroral Sounding System; Milan et al., 1997) radar located in Finland was used to detect stimulated field perpendicular scatter while, simultaneously, the EISCAT UHF radar was observing the quasi-isotropic scatter. The experimental geometry is described in the next section.

Correspondence to: R. S. Dhillon
(rsd6@ion.le.ac.uk)

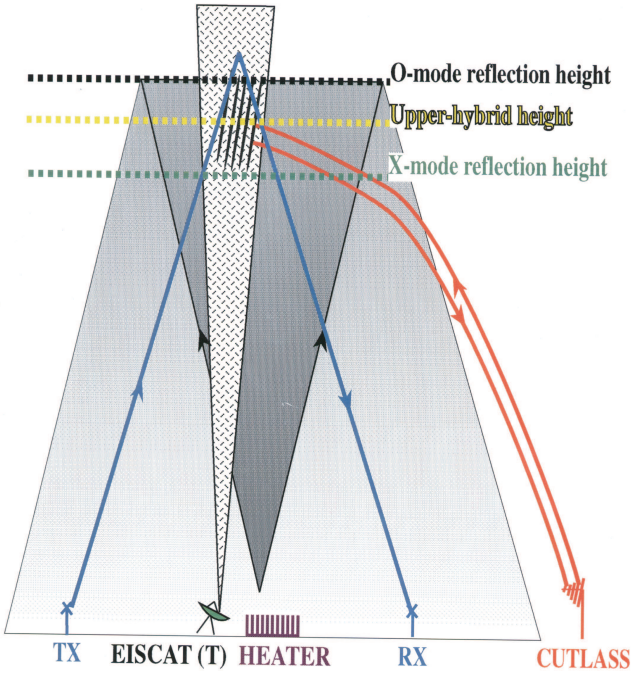

Fig. 1. The experimental setup of the instruments required to modify the ionosphere and to determine plasma parameters. The CUTLASS coherent scatter radar detects heater-enhanced, field-orthogonal backscatter from FAIs. The EISCAT incoherent scatter radar measures heater-enhanced almost-field-parallel backscatter and the electron and ion temperatures.

2 Instrumentation and experimental configuration

The EISCAT (European Incoherent SCATter) ionospheric high-power facility (heater) is situated at Ramfjordmoen, near Tromsø in Norway, and has been operational since the early 1980s (Rietveld et al., 1993). The heater transmits electromagnetic radiation at frequencies of 4–8 MHz with an effective radiated power of up to several hundred MW. Both X- and O-mode-polarized radiation can be transmitted and the signal can be modulated at a wide range of frequencies.

The EISCAT UHF incoherent scatter radar (Rishbeth and Williams, 1985) is collocated with the heater and has been operational since 1981. It is used to determine ionospheric plasma parameters, using a variety of observing modes and pulse schemes, for both background and heater-excited cases. The data presented in this paper were obtained using two pulse schemes that measured the backscatter power and the ion and electron temperatures. A short pulse gives "power-profile" data and is used to measure the backscatter power. The data are collected from altitudes of 75–435 km and have an independent range resolution of 3 km, although over-sampling the signal allows a range resolution of 1.5 km. A "long-pulse" provides ion and electron temperatures from 160-745 km with a range resolution of 22.5 km. Both power-profile and long-pulse data are used to diagnose heater-induced effects and both types of UHF data were collected at 5-s resolution. The EISCAT UHF radar operates at 931 MHz and is thus sensitive to 16 cm wavelength plasma waves. In the experiments described below, the EISCAT UHF backscatter power integrated over the whole ion-line was used as an indicator of enhanced UHF scatter (EUS) caused by the heater.

The 16-beam coherent scatter radar situated at Hankasalmi, Finland, is one of two CUTLASS radars and the heater/UHF site lies within the field-of-view of beam 5. Each beam has a frequency-dependent azimuthal angular width of 3–5°. Heater-induced field-aligned plasma structures are observed using a 1-s-resolution mode with 15-km range gates. The Hankasalmi radar is used to obtain irregularity backscatter data simultaneously with the UHF data. CUTLASS receives scatter from many altitudes, including those at which the irregularities are generated. The CUTLASS radar operates at frequencies between 8 and 20 MHz and is thus sensitive to plasma irregularities with wavelengths between 7 and 19 m.

EISCAT EUS (enhanced UHF scatter) features were examined during experiments undertaken in September 2002. These experiments utilized the ability to orient the UHF in azimuth and elevation. Five pointing directions in the magnetic meridian plane were used. These were field-aligned (FA), 6° and 12° closer to vertical than field-aligned (respectively, FA+6 and FA+12), and 6° and 12° further from vertical than field-aligned (respectively, FA−6 and FA−12). The experiments were conducted on 25 and 26 September 2002 and comprised transmissions of an O-mode 2-min-on/2-min-off heater cycle at radio frequencies of 7.1 MHz. Heating array 1 was used during the experiment and the effective radiated power (ERP) varied from approximately 600–900 MW. This corresponds to an antenna gain of about 28–30 dB. The −3 dB beam width was approximately 6–7°. Four hours of UHF data were taken on each day, between 12:00 and 18:00 UT, in two 2-h blocks, one of which was during sunlit conditions and the other was around dusk. On 25 September the heater pointed solely field-aligned, whereas on 26 September the heater alternated between pointing vertically and field-aligned. The UHF observed for 4 min along each of the five pointing directions, going from FA to FA+6, then FA−6, FA+12 and FA−12, thus completing a 20-min cycle. This cycle was always utilized, regardless of the pointing direction of the heater. The change of UHF pointing direction always occurred during the final 30 s of the 4-min heater cycle of 2-min-on/2-min-off. This meant that the UHF was ready to observe heating effects in its new pointing direction when the heater was switched on and began a new 2-min-on/2-min-off cycle. The EISCAT UHF radar was also used to monitor the background electron density and temperature profiles parameters during the heating experiments. Figure 1 is a schematic representation of the configuration of the heater, UHF and CUTLASS Finland, which is situated approximately 1000 km south of the EISCAT site.

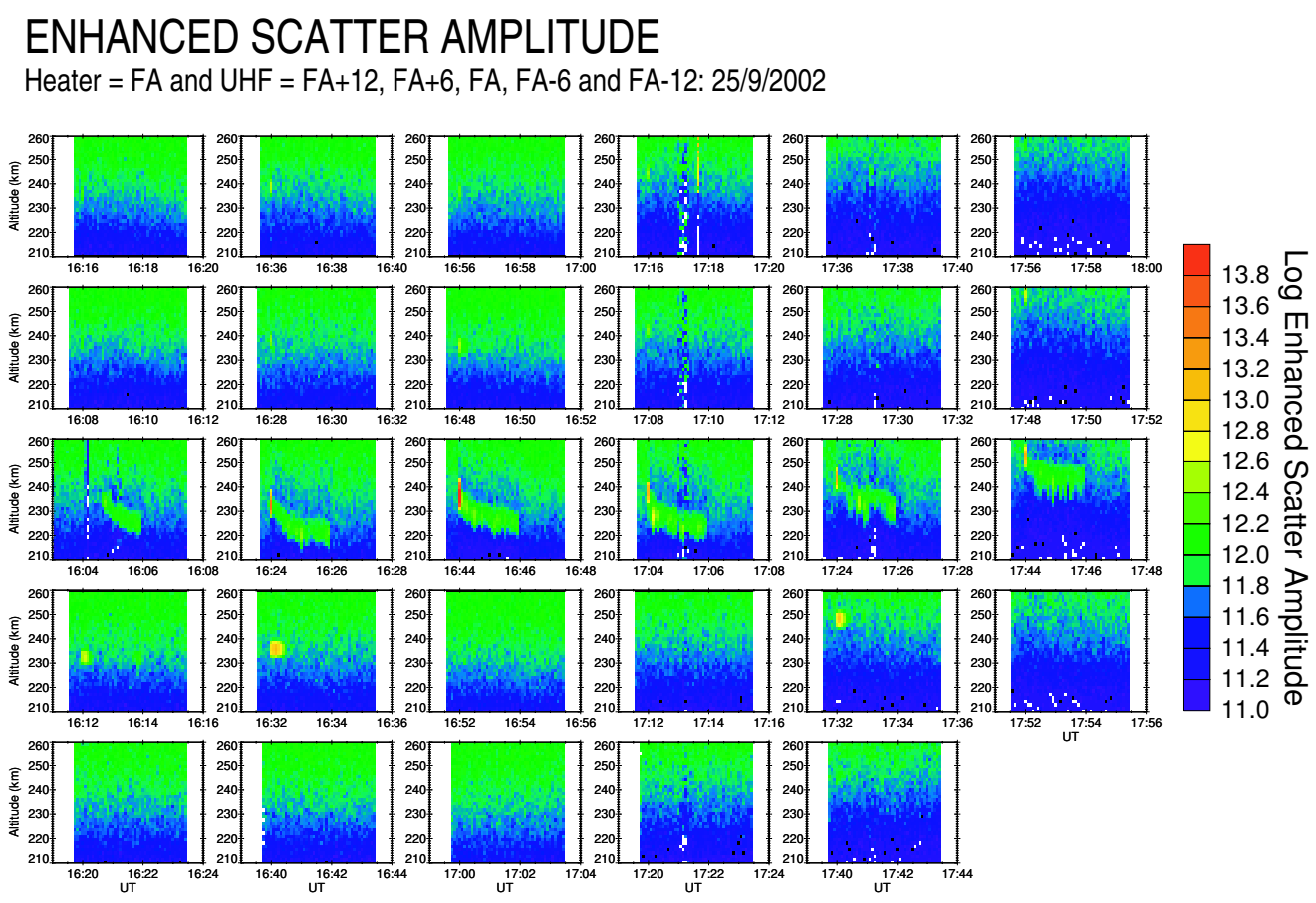

Fig. 2. Backscatter amplitudes for 16:00–18:00 UT on 25 September 2002 for FA heater pointing. The five rows correspond to the five UHF pointing directions: FA+12, FA+6, FA, FA−6 and FA−12. The altitude versus the time is shown and the colours give the backscatter intensity. The backscatter enhancement at heater switch-on may be seen in FA+12, FA+6 and FA, together with a more complex signature in FA−6. For FA UHF pointing, there is a descending signature with backscatter amplitudes that are lower than those at heater switch-on. The descent stabilizes and is present for the entire heater-on interval.

3 EISCAT EUS data

Figures 2, 3 and 4 show the backscatter amplitude for all five UHF pointing directions. The data are separated according to the UHF pointing direction and are shown with the altitude plotted against the time. From top to bottom, the five rows of panels show data from FA+12, FA+6, FA, FA−6 and FA−12. Each panel in a particular row shows the logarithm to base 10 of the backscatter amplitude for one period of heater-on/heater-off when the UHF was pointing in that particular direction. The colour scheme indicates the UHF backscatter amplitude with a scale of 11–14. Figure 2 shows data taken on 25 September for 16:00–18:00 UT, when the heater was transmitting O-mode radiation at 7.1 MHz and was pointing field-aligned. Figure 3 shows data taken on 26 September for 12:00–18:00 UT, when the heater was transmitting O-mode radiation at 7.1 MHz and pointing field-aligned. Figure 4 corresponds to the same interval as that for Fig. 3, but with the heater pointing vertically instead of field-aligned.

In order to determine the background conditions for the data shown in Fig. 2, the UHF pointed FA from 16:00–16:04 UT. The repeated 20-min UHF cycle began at 16:04 UT. The heater performed a continuous-wave tune at 16:05–16:06 UT and then transmitted the 2-min-on/2-min-off heater cycle from 16:08–18:00 UT. The EUS corresponding to heater switch-on may be seen for most UHF pointing directions but not in FA−12. The EUS is only seen in the first 5-s data dump in FA+12, FA+6 and FA. When the UHF pointed FA−6, EUS could not be seen for the heater switch-ons at 16:52, 17:12 and 17:52 UT. For the heater switch-ons at 16:12, 16:32 and 17:32 UT, there was a signature that lasted for several data dumps. For the heater switch-on at 16:12 UT, the signature reappeared at just before 16:14 UT, when the heater was switched off. The EUS observed in FA−6 has an altitudinal spread of approximately 5–7 km. For FA pointing of the UHF, descending EUS, in addition to that for heater switch-on, is present. It is seen throughout the period of heater-on and gradually descends by 10–15 km, reaching the lowest altitude approximately 60 s after heater switch-on. The subsequent EUS amplitude is an order of magnitude less than that at heater switch-on and varies during the period that the heater remains on. The altitudinal spread of the EUS in FA is about 10 km.

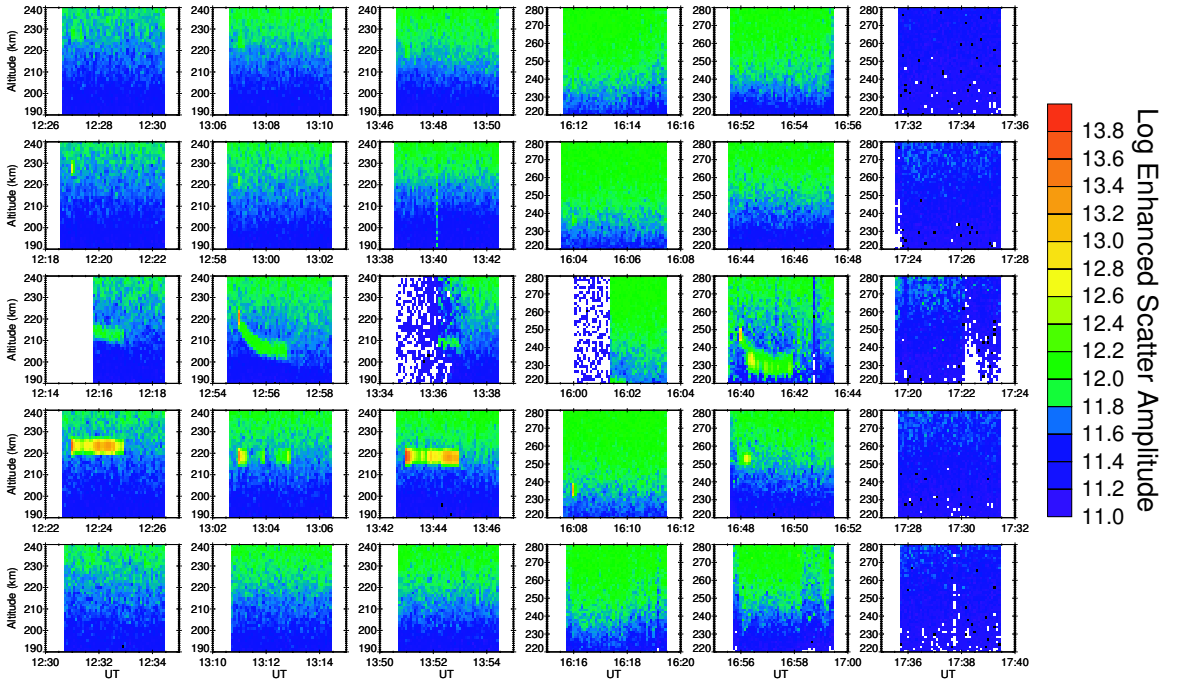

Fig. 3. Backscatter amplitudes for 12:00–18:00 UT on 26 September 2002 for FA heater pointing. The data are shown in the same format as for Fig. 2. The descending signature in FA is again present. There is also a persistent signature in FA−6. This signature is characterized by EUS that does not descend and whose amplitude remains high throughout the on period.

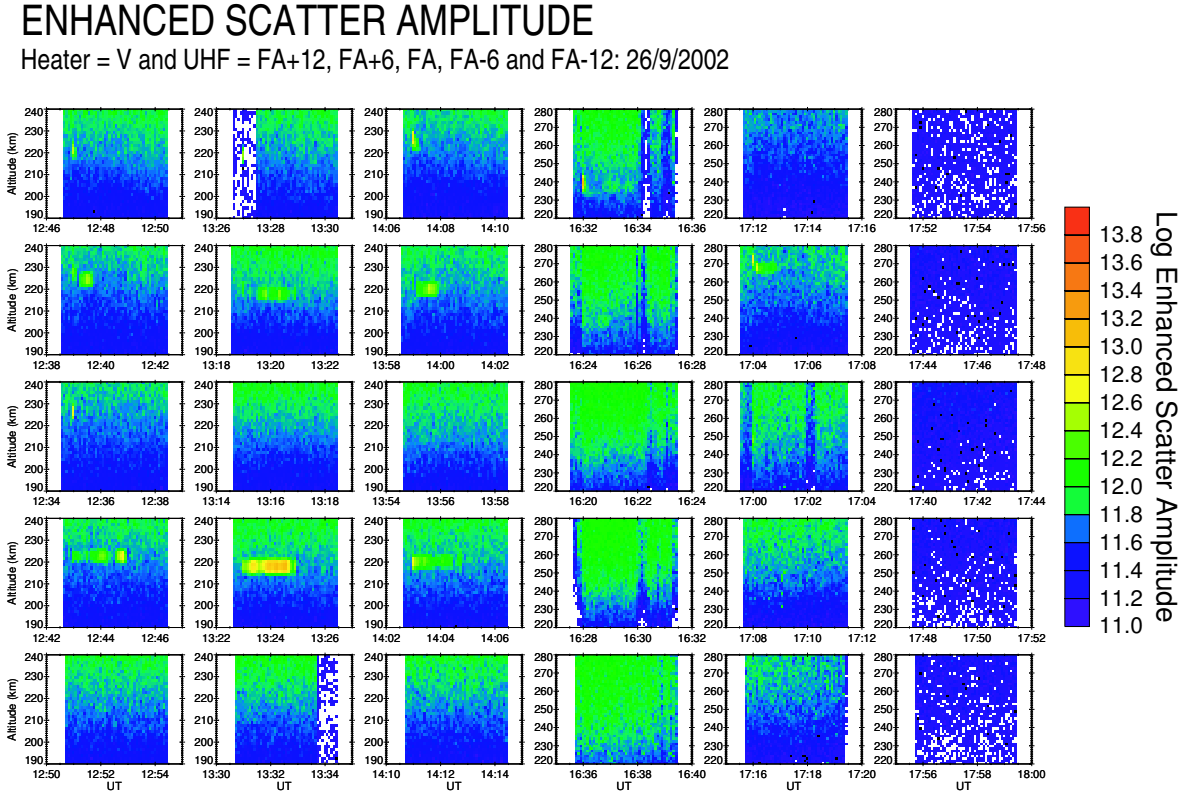

Fig. 4. Backscatter amplitudes for 12:00–18:00 UT on 26 September 2002 for vertical heater pointing. The data are again shown in the format used for Figs. 2 and 3. The persistent signature in FA−6 is also present in this data and has the same characteristics. Only the initial heater-induced backscatter enhancement can be seen in FA. For FA+12, there are signs consistent with a gradual descent, whereas for FA+6, there is a signature whose amplitude is variable throughout the on period.

For Figs. 3 and 4, the lack of data from around 17:30 UT onwards for all directions corresponds to falling background electron concentration and underdense heating. In Fig. 3, the EUS corresponding to heater switch-on is again present for FA+12, FA+6 and FA. The descending signature, characterized by strong initial EUS followed by subsequently weaker descending EUS, is again present for FA. An additional feature may be seen for FA−6 and this is clear in the data for the heater switch-ons that occurred at 12:23 and 13:43 UT. There is an EUS signature at heater switch-on and the subsequent EUS amplitude remains comparable to the initial amplitude throughout the period that the heater remains on. Also, the altitude of the EUS remains steady throughout the 2-min-on period. The EUS corresponding to heater switch-on is present at 13:03 UT, and the signature appears intermittently for the rest of the on period. The switch-on at 16:08 UT is characterized by EUS, with no other features, whereas that at 16:48 UT shows a feature that remains for several data dumps. To summarize, the data for FA−6 may be characterized by large, persistent EUS amplitudes that occur at a fairly constant altitude. This contrasts with the data for FA pointing, which are characterized by high initial amplitudes followed by subsequently weaker descending signatures.

For vertical heater pointing, as shown in Fig. 4, there is again an absence of any significant signature for FA−12. For FA UHF pointing the only signature present is that of the initial EUS and this is only seen occasionally. For FA+12, a slight descent in the EUS after heater switch-on may be seen. An example of this occurs for the switch-on at 14:07 UT. For FA+6, the initial EUS is followed by an additional feature that occurs a few kilometres below it. The amplitude of this additional feature is comparable to that at switch-on and it appears intermittently throughout the on period. As for the data from FA−6 in Fig. 3, there is a non-descending signature in this direction whose amplitude remains high throughout the on period. For the heater switch-on at 12:43 UT, the amplitude of the signature varies throughout the on period and is actually highest approximately 30 s prior to switch-off. The EUS for the heater switch-on at 14:03 UT gradually disappears and the altitude at which the signature is seen remains fairly constant.

4 EISCAT electron temperatures

Figures 5, 6 and 7 show long-pulse electron temperatures corresponding to the EUS data shown in Figs. 2, 3 and 4, respectively, and the data times of the panels correspond to the times in the EUS data. The electron temperature data are also classified according to the five UHF pointing directions. The data are coloured according to temperature, with a scale from 0–5000 K. The data for altitudes below about 190 km had low signal-to-noise ratios and the analysis did not produce reliable results. Figure 5 shows electron temperatures for 16:00–18:00 UT on 25 September. The background electron temperature was approximately 1000–1500 K at the O-mode reflection height. When the heater was switched on, the typical temperature for FA+12, FA+6 and FA−12 was about 2000 K at the interaction height. For FA−6, there are instances where the electron temperature rises to 3000–4000 K for some heater-on intervals. For FA pointing, the highest temperature increase occurs at altitudes from 200–240 km, where the electron temperature increases to over 5000 K. This increase is present for the entire interval that the heater remained on and at altitudes up to approximately 40 km above the interaction height.

Figure 6 shows electron temperatures corresponding to the EUS data shown in Fig. 3. These were high along FA−6 for FA heater pointing, occasionally reaching in excess of 5000 K. The increase in electron temperature could be seen from about 180–250 km. For FA heater pointing, the temperatures for FA UHF pointing were also high, with values from 3000 to in excess of 5000 K. The temperature increases in other directions were not as high. The rise in the field-aligned electron temperature on both days is consistent with the results found by Rietveld et al. (2003), where the aspect sensitivity of heating effects was investigated and evidence suggesting strong field-aligned electron temperature rises was presented.

Figure 7 shows electron temperatures corresponding to the EUS data shown in Fig. 4. There is much more variability for this data with increases present for FA+12, FA+6 and FA−6. For FA+12 and FA+6, the temperature rose to 3000–3500 K. In FA−6, for vertical heater pointing, the values became greater than 5000 K. No noticeable temperature increases were present in FA and FA−12. This apparent lack of dependence of the electron temperature increases on the angle between the radar beam and the geomagnetic field is contrary to the results of Rietveld et al. (2003).

5 CUTLASS coherent scatter data

During the intervals that the EISCAT UHF was collecting data, CUTLASS Finland was also observing the same region of the ionosphere. It typically operated at frequencies of around 19.5 MHz, occasionally dropping to 16 MHz. As shown by Yeoman et al. (2001) in a study on the propagation of the radar radio waves, there is little refraction at these frequencies and rectilinear propagation of the radio waves may be assumed.

The upper panel of Fig. 8 shows data collected during the period from 16:00–18:00 UT on 25 September 2003. The 2-min-on/2-min-off heater signature is clear in the CUTLASS data, with unusually weak backscatter powers of 20 dB being seen. These are considerably lower than the powers of 40–50 dB that have often been observed previously. The range gates in which the data occurred are shown on the left-hand axis, with the corresponding slant range shown on the right-hand axis. The heater was pointing FA throughout and the positions of the five UHF pointing directions calculated at the interaction altitude are overlaid on the data. The five horizontal black lines, with decreasing range gate and slant

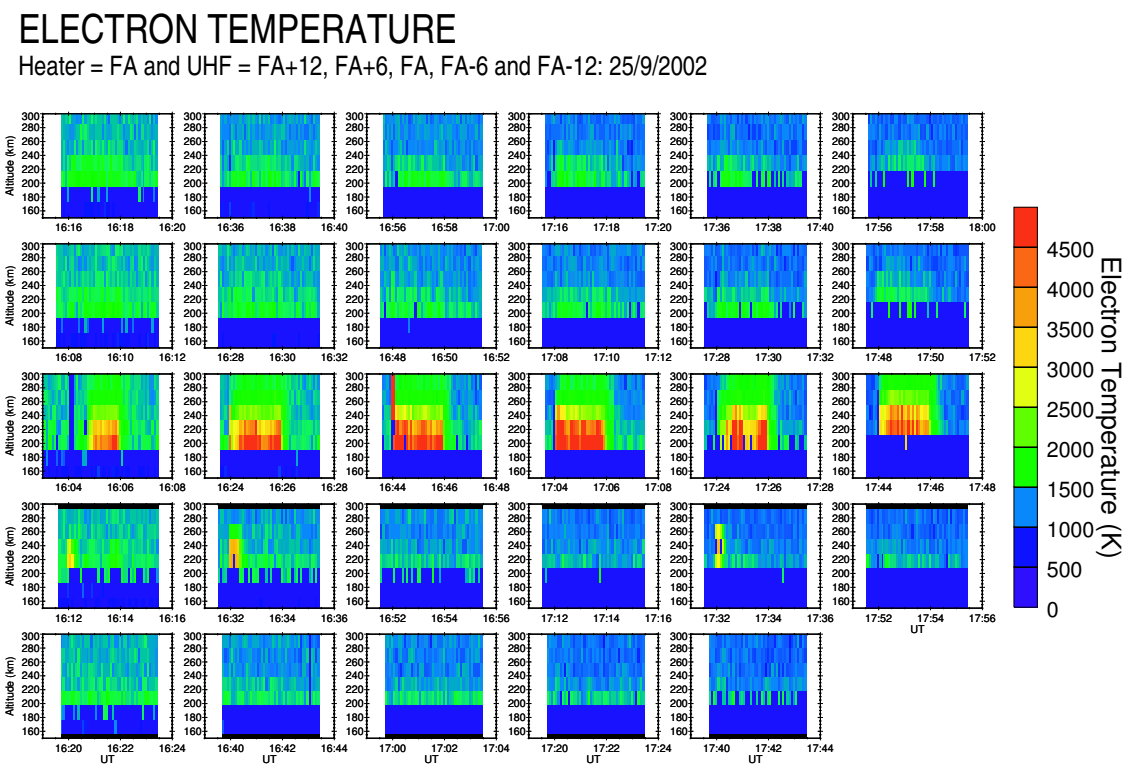

Fig. 5. Electron temperatures for 16:00–18:00 UT on 25 September 2002 for FA heater pointing. The five rows correspond to the five UHF pointing directions: FA+12, FA+6, FA, FA−6 and FA−12. Each panel shows the altitude plotted against the time, with the colours corresponding to the electron temperature. Temperature increases corresponding to heater-on are present in most directions. The highest increases are in FA, with temperatures up to 5000 K. The increased temperature persists for the entire period that the heater remains on.

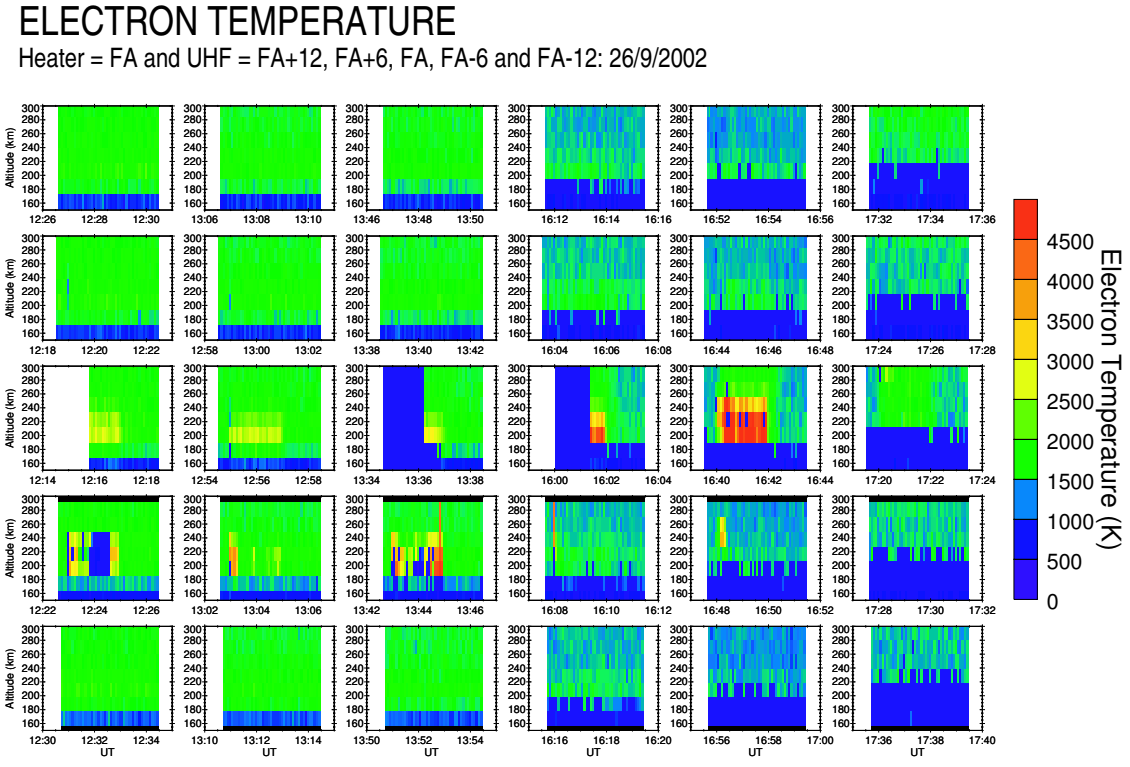

Fig. 6. Electron temperatures for 12:00–18:00 UT on 26 September 2002 for FA heater pointing. The data are shown in the same format as for Fig. 5. Significant temperature increases, with values in excess of 5000 K, corresponding to heater-on are present for FA and FA−6.

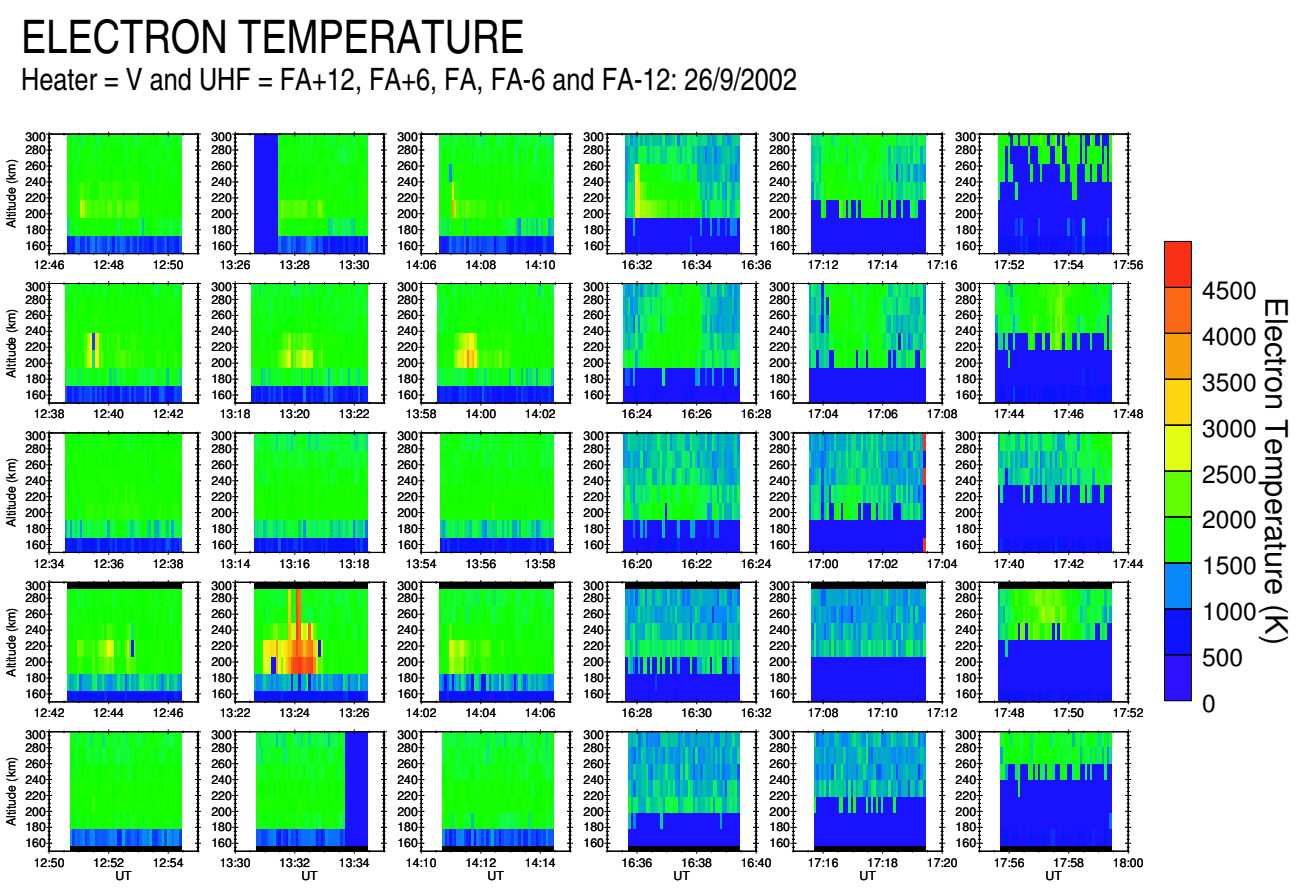

Fig. 7. Electron temperatures for 12:00–18:00 UT on 26 September 2002 for vertical heater pointing. The data are again shown using the format used for Figs. 5 and 6. There is much more variability in this data. Significant temperature increases, with values in excess of 5000 K, corresponding to heater-on are present for FA−6. There are also signatures in FA+6. No signature is present in FA.

range, correspond to FA+12, FA+6, FA, FA−6 and FA−12, respectively.

The strongest signature is for FA pointing of the UHF. There is much weaker scatter in the regions corresponding to the other observation directions of the UHF. The central panel shows data from 12:15–14:15 UT on 26 September 2003, when the heater alternately pointed vertically and FA. The scatter is strongest from the regions excited by the centre of the heater beam, for either vertical or FA heater pointing, with much weaker scatter from other regions. The lower panel shows data from 16:00–18:00 UT on 26 September 2003. There were significant backscatter powers corresponding to the heater pointing direction for the period from 16:00–17:30 UT, and these are higher than those measured from 12:15–14:15 UT.

6 Analysis of altitude and intensity of EUS

By inspection, the descending signatures for FA heater and UHF pointing appeared to have approximately exponential forms for the altitude decrease. Therefore, the descending EUS signatures were examined quantitatively in order to determine the closeness of their functional form to that of an exponential. Figure 9 shows data from four heater switch-ons, at 16:24, 16:44, 17:04 and 17:24 UT on 25 September, and the subsequent 5-s-resolution EUS maxima until heater switch-off. The data are plotted with the logarithm of the altitude shown against the time. The logarithm of the backscatter amplitude is again used to indicate the intensity. The figure shows the results of fitting straight lines to the data. These represent the functional form $\Delta h e^{-t/\tau}$, where Δh is the maximal altitude decrease from heater switch-on, at t=0, to when the altitude variation has stabilized, for $t \rightarrow \infty$. The fit is generally good and shows that the form of the descent is approximately exponential.

Consecutive altitude profiles of the EUS signatures corresponding to a single heater-on period are shown in Fig. 10. Each panel of the figure, from left to right and then down the page, corresponds to a single 5-s data dump. The data are taken from 16:24–16:26 UT on 25 September when the heater and UHF were pointing field-aligned. The altitude profiles of the data are apparently Gaussian. Consequently, Gaussians were fitted to the altitude profiles in order to determine their closeness to a Gaussian form. In each panel, the green line shows the data, for the altitude range 215–245 km, and the red line gives the values for the fitted Gaussian. The fitted values correspond well with the data, with the maxi-

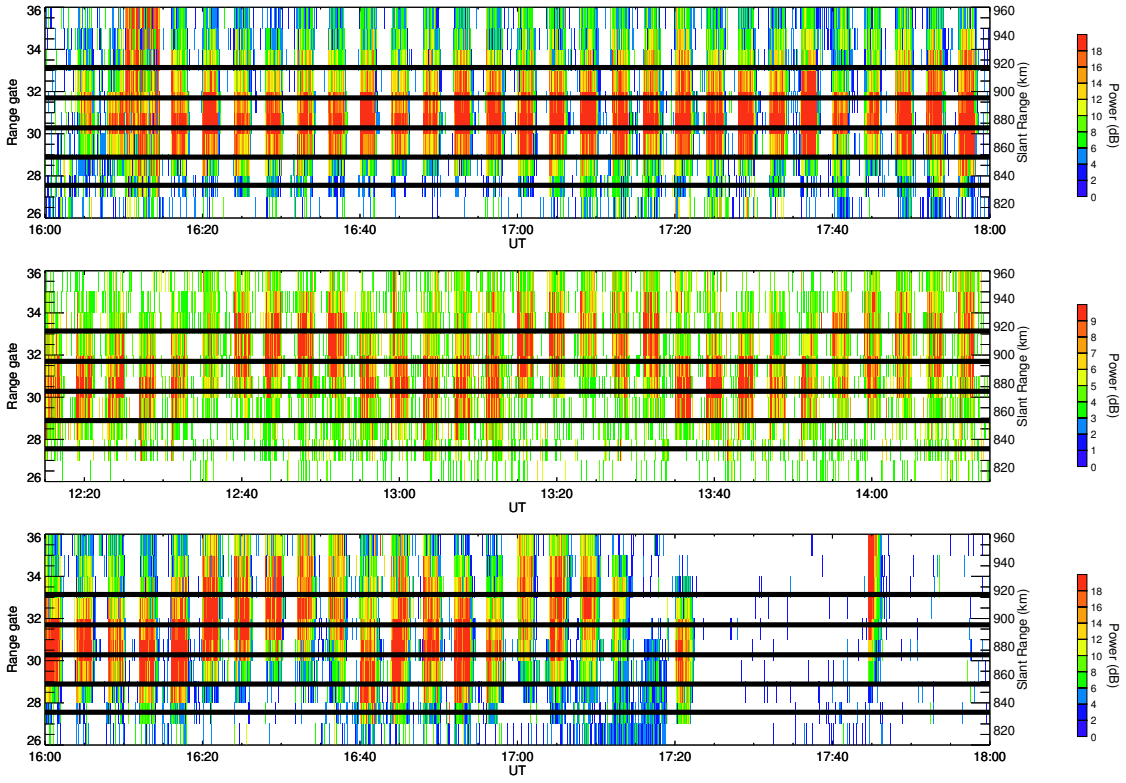

Fig. 8. CUTLASS backscatter powers, together with overlaid UHF positions, obtained for (**a**) 16:00–18:00 UT on 25 September 2002, (**b**) 12:15–14:15 UT on 26 September 2002 and (**c**) 16:00–18:00 UT on 26 September 2002. The UHF positions FA+12, FA+6, FA, FA−6 and FA−12 are shown using the horizontal yellow lines and correspond to decreasing range gate and slant range. The backscatter powers are only high in the directions in which the heater points, vertical and field-aligned.

mum occurring at the O-mode reflection height. The Gaussian full-width-at-half-maximum is approximately 6 km and the data signature has an altitudinal extent of approximately 12 km.

7 Discussion

In this study, the aspect sensitivity of heater-enhanced ion-line scatter was investigated for heater pointing directions of field-aligned and vertical. The scatter data were collected by the UHF radar from five equally spaced directions in the magnetic meridian plane, centred at field-aligned. The EUS data for field-aligned heater and UHF pointing contained a descending signature that was present during the entire heater-on period and which disappeared when the heater was switched off. The FA−6 EUS data contained a signature that did not descend and which was present during the entire heater-on period. For the entire heater-on period, the altitudinal extent of both types of signature was approximately 6–12 km. The altitude profile was approximately Gaussian for the FA signature but was more flattened for the FA−6 signature. For the FA signature, the EUS amplitude decreased rapidly after heater switch-on and then remained fairly constant. For FA−6, the EUS amplitude remained comparable to that at heater switch-on. The heater-induced EISCAT electron temperature increases were also anisotropic. This is highlighted by the case of field-aligned heater pointing, where the highest temperature increases were recorded for field-aligned pointing of the UHF. The increases in other directions were not as pronounced. In particular, the electron temperatures in FA−6 were not significantly different from those in FA+12 and FA+6. For vertical heating, the temperature increases were lower and were not as clear as those for field-aligned heater and UHF pointing

The intensity of the field-perpendicular scatter observed by CUTLASS was highest for the area of the ionosphere excited by the central part of the heater beam, with low intensities in other areas. The heated patch was approximately 100 km wide. The upper-hybrid height, where irregularity generation is thought to occur (Robinson, 1989), lay about 5 km below the O-mode reflection height for vertically propagating heater waves. The FA−6 and FA−12 data are consistent with reflection of the heater waves below the

upper-hybrid height, as the reflection heights were 10 and 15 km below the upper-hybrid height, respectively. The standard simple mechanism for irregularity generation requires the heater radio waves to attain altitudes higher than that of the upper-hybrid height. Under simple considerations, there are severe constraints on the development of irregularities for heater pump propagation directions sufficiently far from vertical that the heater waves ought not to be able to reach the upper-hybrid height (Mishin et al., 2004). It is worth noting that irregularities have been observed with CUTLASS on many occasions when this simple condition has been violated.

Additionally, it should be noted that heater-induced lower-hybrid waves have perpendicular wavelengths of the order of 1–10 m. These could enhance the backscatter observed by CUTLASS, although this scatter is expected to be weaker than that from irregularities. Furthermore, modelling undertaken by Blaunstein (1997) shows that irregularities within the heated patch could be generated by the gradient-drift instability. Also, Landau damping may cause the amplitude of the waves in FA to decrease if the heating is produced by, for example, invisible upper hybrid waves.

Many EISCAT studies of EUS have focused upon plasma-line scatter (e.g. Kohl et al., 1993; Isham et al., 1999). These include the time-history study of Djuth et al. (1994), who, mainly for vertical heater and UHF pointing, observed a persistent signature that descended by about 3 km and whose amplitude was lower than that at heater switch-on. The 1-min-on/2-min-off heater cycles were used, with a typical heater frequency of 6.77 MHz. Plasma-line EUS was observed for the entire heater-on period and the lowest EUS altitude occurred 30 s after heater switch-on. Djuth et al. (1994) explained the descending EUS by enhanced electron concentration caused by reduced recombination due to the temperature increases. The recombination coefficient is a decreasing function of temperature (Biondi, 1969) and hence higher temperatures increase the level of reduced recombination. This is consistent with the results of Gurevich (1978), Jones et al. (1982) and Robinson (1989), and also with Honary et al. (1993), who found that chemical processes dominated over transport effects at lower altitudes. EUS amplitude reductions after heater switch-on have been explained using energy diversion from reflection height instabilities caused by artificial field-aligned irregularities (FAIs) and anomalous absorption (Robinson et al., 1996).

In addition to studying the heater-enhanced plasma-line, Isham et al. (1999) also measured the heater-enhanced ion-line as a function of the UHF pointing direction, including FA. Their study was performed with a low duty cycle, probably creating fewer irregularities, a lower frequency and a wider heater beam. This probably resulted in a narrower excitation region than that for the present study.

Djuth et al. (1994) observed descent in the vertical direction and in the direction given by tilting the heater beam 5° away from vertical towards the south. The study described in this paper highlighted descent in FA. Other data signatures were seen in directions away from FA and the anisotropic

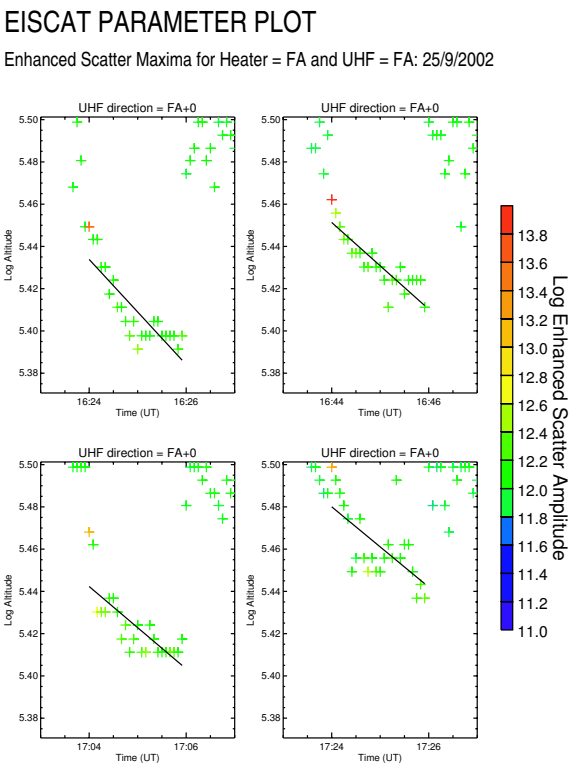

Fig. 9. The logarithm of the altitude plotted against the time, for FA heater and UHF pointing. Four cases are shown. The fit was performed in order to attempt to characterize the electron concentration increases using an exponential function. There is good agreement between the fitted lines and the data.

nature of the EUS data is clear. The high heater-induced electron temperature increases and the lowering of the reflection height, although seen in the present study in FA, are consistent with the results of Djuth et al. (1994). The high temperatures are probably caused by enhanced heating in the field-aligned direction. In addition to their possibly reducing the EUS amplitude via anomalous absorption, FAIs generated as heating progresses may also act as waveguides and channel the heater-induced ion-acoustic waves in the field-aligned direction. The guiding process may operate by focusing along the geomagnetic field those waves whose wave vectors are generally parallel to it. The observed EUS may therefore be concentrated, and persistently observed, close to the field-aligned direction. Also, FAI generation is consistent with the EUS amplitude reduction for FA UHF pointing after heater switch-on. The heater did not excite FAIs as strongly in FA−6, as indicated by the CUTLASS data, and hence associated anomalous absorption was not as strong as for when irregularities were present (Honary et al., 1995; Robinson et al., 1996). This is consistent with the high EUS amplitude during the period that the heater remained on (Honary et al., 1999).

A number of features remain unexplained, however. The high electron temperatures in FA−6 suggest that descent ought to occur in this direction. This is not in agreement with

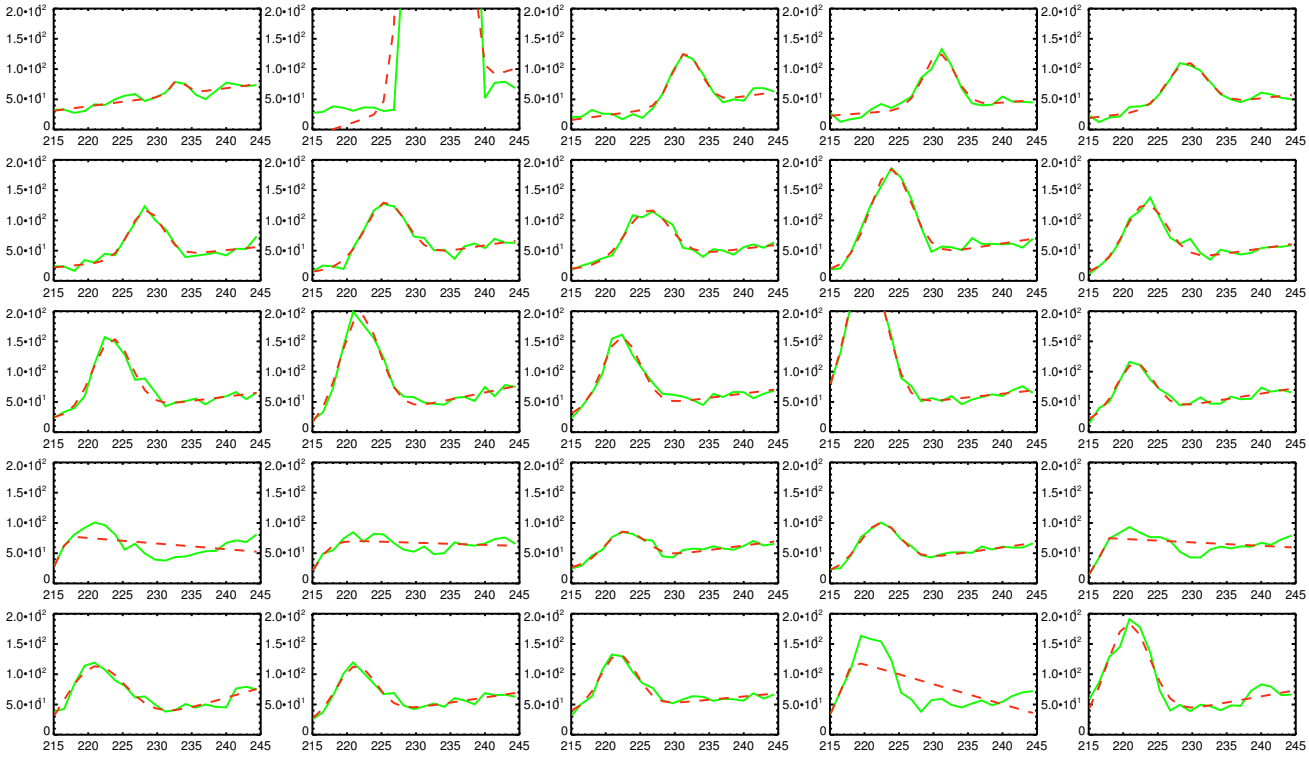

Fig. 10. The altitude profiles of the data for successive 5-s data from just before heater switch-on to heater switch-off. Chronological order is given by going from left to right and then down the page. In each panel, the data are shown using a solid green line and a fitted Gaussian profile is shown using a dashed red line. There is very good agreement between the data and the fitted Gaussian.

the almost constant altitude of the FA−6 EUS. For FA heater pointing, the reason for the absence of a similar signature in FA+6 to that in FA−6 is unknown. Both directions are 6° away from FA and the observed irregularity amplitudes were low for both FA+6 and FA−6. For vertical heater pointing, the lack of significant EUS in FA, given the signatures for FA+6 and FA−6, is also difficult to explain. Finally, the importance of FA−6, in which persistent non-descending EUS is seen for both vertical and FA heater pointing, remains unclear.

Jones et al. (1982) observed exponential forms for the electron concentration enhancements, ΔN_e, during earlier EISCAT heating experiments, with time constants of around 30–40 s. Applying Jones et al.'s (1982) electron-concentration-dependent expression for the time constant to the present data gives it as 25 s. The time constant obtained directly from the descending EUS signatures by functional fitting is approximately 30 s. These values of 25 and 30 s are consistent with those of Jones et al. (1982). ΔN_e was obtained from the EUS data at the altitude at which the descent stabilized. The electron concentration at heater switch-on was subtracted from that corresponding to stabilization of the altitude change. The highest value of ΔN_e was typically $2\times10^{11}\mathrm{m}^{-3}$. This implies $\Delta N_e/N_e\approx$40%, which is significantly larger than has been reported previously (e.g. Jones et al., 1982; Rietveld et al., 2003). High $\Delta N_e/N_e$ is consistent with large ΔT_e, the electron temperature change. $\Delta T_e>$2000 K, corresponding to $\Delta T_e/T_e>$ 100%, was frequently seen.

In conclusion, the generally anisotropic nature of the observed heater-enhanced UHF backscatter is consistent with the presence of field-aligned irregularities. This is particularly true for possible field-aligned damping of ion-acoustic waves. This study has provided tentative evidence for field-aligned irregularities influencing the excitation and propagation of heater-induced ion-acoustic waves. Also, the descending EUS signatures have indicated the importance of temperature-dependent chemical effects in determining F-region electron concentration characteristics.

Acknowledgements. Many thanks are due to the EISCAT Scientific Association, M. Rietveld, for operating the Tromsø heater and providing useful technical information, and the EISCAT group at the Rutherford Appleton Laboratory. The authors would also like to thank E. Mishin for helpful discussions. CUTLASS is supported by the Particle Physics and Astronomy Research Council (PPARC grant no. PPA/R/R/1997/00256) UK, the Finnish Meteorological Institute, Helsinki and the Swedish Institute of Space Physics, Uppsala.

The Editor in chief thanks M. T. Rietveld and another referee for their help in evaluating this paper.

References

Biondi, M. A.: Atmospheric electron-ion and ion-ion recombination processes, Can. J. Chem., 47, 1711–1722, 1969.

Blaunstein, N.: Evolution of a stratified plasma structure induced by local heating of the ionosphere, J. Atmos. Terr. Phys., 59, 351–361, 1997.

Bond, G., Robinson, T. R., Eglitis, P., Wright, D. M., Stocker, A. J., Rietveld, M. T., and Jones, T. B.: Spatial observations by the CUTLASS coherent scatter radar of ionospheric modification by high power radio waves, Ann. Geophys., 15, 1412–1421, 1997, **SRef-ID: 1432-0576/ag/1997-15-1412**.

Coster, A. J., Djuth, F. T., Jost, R. J., and Gordon, W. E.: The temporal evolution of 3-m striations in the modified ionosphere, J. Geophys. Res., 90, 2807–2818, 1985.

Dhillon, R. S., Robinson, T. R., and Wright, D. M.: Radar ACFs and turbulence characteristics from artificially generated field-aligned irregularities, Geophys. Res. Lett., 29, 1830, doi:10.1029/2002GL015364, 2002.

Djuth, F. T., Stubbe, P., Sulzer, M. P., Kohl, H., Rietveld, M. T., and Elder, J. H.: Altitude characteristics of plasma turbulence excited with the Tromsø superheater, J. Geophys. Res., 99, 333–339, 1994.

Gurevich, A. V.: Nonlinear phenomena in the ionosphere, Springer-Verlag, New York, 1978.

Hedberg, Å., Derblom, H., Thidé, B., Kopka, H., and Stubbe, P.: Observations of HF backscatter associated with the heating experiment at Tromsø, Radio Sci., 18, 840–850, 1983.

Honary, F., Stocker, A. J., Robinson, T. R., Jones, T. B., Wade, N. M., Stubbe, P., and Kopka, H.: EISCAT observations of electron temperature oscillations due to the action of high power HF radio waves, J. Atmos. Terr. Phys., 55, 1433–1448, 1993.

Honary, F., Stocker, A. J., Robinson, T. R., Jones, T. B., and Stubbe, P.: Ionospheric plasma response to HF radio waves operating at frequencies close to the third harmonic of the electron gyrofrequency, J. Geophys. Res., 100, 21 489–21 501, 1995.

Honary, F., Robinson, T. R., Wright, D. M., Stocker, A. J., Rietveld, M. T., and McCrea, I.: First direct observations of the reduced striations at pump frequencies close to the electron gyroharmonics, Ann. Geophys., 17, 1235–1238, 1999, **SRef-ID: 1432-0576/ag/1999-17-1235**.

Isham, B., Rietveld, M. T., Hagfors, T., La Hoz, C., Mishin, E., Kofman, W., Leyser, T. B., and van Eyken, A. P.: Aspect angle dependence of HF enhanced incoherent backscatter, Adv. Space Res., 24, 1003–1006, 1999.

Istomin, Ya. N. and Leyser, T. B.: Parametric decay of an electromagnetic wave near electron cyclotron harmonics, Phys. Plasmas, 2, 2084–2097, 1995.

Jones, T. B., Robinson, T. R., Kopka, H., and Stubbe, P.: Phase changes induced in a diagnostic radio wave passing through a heated region of the auroral ionosphere, J. Geophys. Res., 87, 1557–1564, 1982.

Kolesnikova, E., Robinson, T. R., and Davies, J. A.: Predicted and observed characteristics of small-scale field-aligned irregularities generated in the F-region by low power HF heating, Ann. Geophys., 20, 647–653, 2002, **SRef-ID: 1432-0576/ag/2002-20-647**.

Kohl, H., Kopka, H., Stubbe, P., and Rietveld, M. T.: Introduction to ionospheric heating at Tromsø-II. Scientific problems, J. Atmos. Terr. Phys., 55, 601–613, 1993.

Milan, S. E., Yeoman, T. K., Lester, M., Thomas, E. C., and Jones, T. B.: Initial backscatter occurrence statistics from the CUTLASS HF radars, Ann. Geophys., 15, 703–718, 1997, **SRef-ID: 1432-0576/ag/1997-15-703**.

Mishin, E. V., Burke, W. J., and Pedersen, T.: On the onset of HF-induced airglow at HAARP, J. Geophys. Res., 109, A02305, doi:10.1029/2003JA010205, 2004.

Rietveld, M. T., Kohl, H., Kopka, H., and Stubbe, P.: Introduction to ionospheric heating at Tromsø-I. Experimental overview, J. Atmos. Terr. Phys., 55, 577–599, 1993.

Rietveld, M. T., Isham, B., Kohl, H., La Hoz, C., and Hagfors, T.: Measurements of HF-enhanced plasma and ion lines at EISCAT with high-altitude resolution, J. Geophys. Res., 105, 7429–7439, 2000.

Rietveld, M. T., Kosch, M. J., Blagoveshchenskaya, N. F., Kornienko, V. A., Leyser, T. B., and Yeoman, T. K.: Ionospheric electron heating, optical emissions and striations induced by powerful HF radio waves at high latitudes: aspect angle dependence, J. Geophys. Res., 108, 1141, doi:10.1029/2002JA009543, 2003.

Rishbeth, H. and Williams, P. J. S.: The EISCAT ionospheric radar: the system and its early results, Q. Jl R. astr. Soc., 26, 478–512, 1985.

Robinson, T. R.: The heating of the high latitude ionosphere by high power radio waves, Phys. Rep., 179, 79–209, 1989.

Robinson, T. R., Honary, F., Stocker, A. J., Jones, T. B., and Stubbe, P.: First EISCAT observations of the modification of F-region electron temperatures during RF heating at harmonics of the electron gyro frequency, J. Atmos. Terr. Phys., 58, 385–395, 1996.

Stubbe, P., Kohl, H., and Rietveld, M. T.: Langmuir turbulence and ionospheric modification, J. Geophys. Res., 97, 6285–6297, 1992.

Yeoman, T. K., Wright, D. M., Stocker, A. J., and Jones, T. B.: An evaluation of range accuracy in the Super Dual Auroral Radar Network over-the-horizon HF radar systems, Radio Sci., 36, 801–813, 2001.